Developmental Cell
Article

# LEAFY Target Genes Reveal Floral Regulatory Logic, *cis* Motifs, and a Link to Biotic Stimulus Response

Cara M. Winter,[1] Ryan S. Austin,[2] Servane Blanvillain-Baufumé,[3] Maxwell A. Reback,[1] Marie Monniaux,[4] Miin-Feng Wu,[1] Yi Sang,[1] Ayako Yamaguchi,[1] Nobutoshi Yamaguchi,[1] Jane E. Parker,[3] Francois Parcy,[4] Shane T. Jensen,[5] Hongzhe Li,[6] and Doris Wagner[1,*]

[1]Department of Biology, University of Pennsylvania School of Arts and Sciences, Philadelphia, PA 19104, USA
[2]Centre for the Analysis of Genome Evolution and Function, University of Toronto, Toronto, M5S 3B2 ON, Canada
[3]Department of Plant-Microbe Interactions, Max-Planck Institute for Plant Breeding Research, 50829 Cologne, Germany
[4]Laboratoire Physiologie Cellulaire et Végétale CNRS, iRTSV/CEA, INRA, UJF Grenoble I, Grenoble, France
[5]Department of Statistics, University of Pennsylvania Wharton School, Philadelphia, PA 19104, USA
[6]Department of Biostatistics, University of Pennsylvania School of Medicine, Philadelphia, PA 19104, USA
*Correspondence: wagnerdo@sas.upenn.edu
DOI 10.1016/j.devcel.2011.03.019

## SUMMARY

**The transition from vegetative growth to flower formation is critical for the survival of flowering plants. The plant-specific transcription factor LEAFY (LFY) has central, evolutionarily conserved roles in this process, both in the formation of the first flower and later in floral patterning. We performed genome-wide binding and expression studies to elucidate the molecular mechanisms by which LFY executes these roles. Our study reveals that LFY directs an elaborate regulatory network in control of floral homeotic gene expression. LFY also controls the expression of genes that regulate the response to external stimuli in *Arabidopsis*. Thus, our findings support a key role for LFY in the coordination of reproductive stage development and disease response programs in plants that may ensure optimal allocation of plant resources for reproductive fitness. Finally, motif analyses reveal a possible mechanism for stage-specific LFY recruitment and suggest a role for LFY in overcoming polycomb repression.**

## INTRODUCTION

Angiosperms or flowering plants are the most successful clade of plants representing nearly 90% of extant land plants. To reach the next generation, flowering plant meristems must cease formation of leaves or branches and initiate formation of reproductive structures, the flowers (Poethig, 2003; Steeves and Sussex, 1989). This requires large-scale alterations in the transcriptional program during the meristem identity transition (Moyroud et al., 2010). This transition also triggers the switch from biomass and resource accumulation in the leaves to allocation of these resources to seed formation. Despite their importance for agriculture and plant reproductive success, the underlying regulatory mechanisms coordinating these events remain to be fully elucidated.

Optimal timing of the meristem identity transition is of particular import in monocarpic (annual) plants such as *Arabidopsis thaliana*, which only flower once in their life. Hence this developmental switch is tightly controlled by both environmental signals such as daylength, temperature, and light (quantity and quality), and by endogenous cues including the age of the plant (Kim et al., 2009; Kobayashi and Weigel, 2007; Komeda, 2004; Turck et al., 2008). These pathways converge to upregulate the expression of meristem identity genes including the plant-specific transcription factor *LEAFY* (*LFY*) (Liu et al., 2009a; Parcy, 2005). LFY is necessary and sufficient for the correct induction of floral fate, and is considered a master regulator of the meristem identity transition (Blazquez et al., 2006; Moyroud et al., 2010; Weigel et al., 1992; Weigel and Nilsson, 1995). Subsequently, LFY directs floral organ patterning by activating floral homeotic gene expression (Krizek and Fletcher, 2005; Weigel and Meyerowitz, 1993).

To gain insight into the regulatory mechanisms coordinating reproductive development, we used chromatin immunoprecipitation coupled with tiling array hybridization (ChIP-chip) and transcriptional profiling to uncover the range of activities and direct transcriptional changes effected by LFY during the meristem identity transition and during flower development.

## RESULTS

### Genomic Regions Bound by LFY at Two Developmental Stages

First, we identified genes bound by LFY during the meristem identity transition in seedlings. Because of the low *LFY* levels present at this early stage (Blazquez et al., 1997) (see Figures S1A and S1B available online), we employed an inducible form of LFY, 35S:LFY-GR, which fully rescues the *lfy* null mutant phenotype (Wagner et al., 1999). We have previously shown that activation of 35S:LFY-GR in 9-day-old wild-type seedlings allows identification of direct LFY target genes with a role in the meristem identity transition (Saddic et al., 2006; Wagner et al., 1999; Pastore et al., submitted; William et al., 2004). After treating 9-day-old 35S:LFY-GR seedlings for 4 hr with

dexamethasone, we immunoprecipitated LFY-DNA complexes using anti-LFY antiserum (Wagner et al., 1999; William et al., 2004) and hybridized the associated DNA fragments to *Arabidopsis* whole-genome tiling arrays (Figure S1B). Using a moving average algorithm (Ji et al., 2008), we identified 1588 significant LFY binding peaks at a false discovery rate of <0.05. Independent validation of enrichment indicates that the FDR is likely lower (Figure S1C). The low signal in control immunoprecipitations, the narrow LFY binding peak width, and the high average ChIP enrichment provide additional evidence for the quality of the ChIP-chip data (Figure S1D). The 1588 binding peaks were associated with 1296 unique genes (see Supplemental Experimental Procedures for details). Six of the seven known direct LFY meristem identity targets were identified by ChIP-chip, including *APETALA1* (*AP1*) and *LATE MERISTEM IDENTITY* 1 (*LMI1*) (Figure 1A; Figure S1E) (Busch et al., 1999; Parcy et al., 1998; Saddic et al., 2006; Wagner et al., 1999; William et al., 2004).

In a second experiment, we identified genes bound by endogenous LFY during floral patterning in 19-day-old wild-type inflorescences bearing young flower primordia using anti-LFY antiserum for ChIP. This analysis uncovered a total of 867 significant LFY binding peaks (FDR < 0.05) and 748 associated unique genes. The quality of this ChIP-chip data set was equivalent to that obtained at the seedling stage (Figure S1). Both of the known floral homeotic LFY target genes *APETALA3* (*AP3)* and *AGAMOUS* (*AG)* (Busch et al., 1999; Lamb et al., 2002) were identified in the inflorescence ChIP-chip (Figure 1A). LFY bound to a promoter proximal region of *AP3* known to be important for proper expression in developing flower primordia and to the previously defined LFY-responsive enhancer in the second intron of *AG* (Busch et al., 1999; Hill et al., 1998).

Comparison of LFY target genes identified at both stages revealed a significant overlap ($p < 10^{-296}$), providing independent validation of a subset of the LFY targets (Figure 1B). This overlap is expected because LFY continues to induce floral fate in incipient primordia in inflorescences (Blazquez et al., 2006). Consistent with a possible role for LFY binding events in transcriptional regulation, binding peaks clustered near transcription start sites (Figure 1C; Table S1).

To determine how frequently LFY binding leads to rapid changes in gene expression, we used the same LFY-GR activation procedure as for ChIP followed by transcriptome analysis. Forty-one percent of the genes bound by LFY at the seedling stage showed rapid changes in gene expression after LFY-GR activation (FDR < 0.05; Figure 1D) with 59% of these gene expression changes being greater than 1.5-fold (Figure S1F). Accordingly, LFY binding increases the probability that a given gene will exhibit altered expression in response to LFY-GR activation ($p < 10^{-16}$, logistic regression; Figure 1E). Some of the remaining LFY targets may require longer periods of LFY induction to show significant expression changes, or may be regulated by LFY only after accumulation of a cofactor not present in our experimental conditions. We observed nearly equivalent roles for LFY in up- and downregulation of gene expression (Figure 1D), in agreement with previous reports that LFY can act as a transcriptional activator and repressor (Parcy et al., 2002; Wagner et al., 1999; William et al., 2004).

## Selection of High-Confidence LFY Target Genes

Next, we identified a high-confidence list of likely physiologically relevant direct LFY target genes from the seedling and inflorescence ChIP-chip data sets using public transcriptome data (Schmid et al., 2003, 2005; Wellmer et al., 2006). Specifically, we selected LFY-bound genes that were significantly differentially expressed in *lfy* mutants relative to wild-type plants (FDR <0.05 and |fold change| >1.5), and that were also strongly coexpressed with endogenous *LFY* (Pearson correlation $p < 0.05$) (see Experimental Procedures for details; Figure S2 and Table S2). Relative to all *Arabidopsis* genes, LFY-bound genes were highly enriched for genes that met these criteria (Fisher's exact $p < 10^{-15}$; Table S2). About one-quarter of the seedling LFY target genes and of the inflorescence LFY target genes were LFY-dependent and *LFY*-coexpressed (Figure 1F). We used only these high-confidence seedling and inflorescence LFY target genes for further analyses.

## LFY Controls Floral Homeotic Gene Expression via an Intricate Regulatory Network

To infer the predicted functions of the high-confidence LFY target genes, we performed Gene Ontology (GO) term analysis (see methods). This revealed strikingly different GO term enrichments ($p < 0.00005$) at the two developmental stages analyzed (Figure 1G). As expected, transcriptional regulators were significantly enriched among the target genes identified at both stages.

The most highly enriched GO terms for inflorescence LFY targets were "organ development" ($p < 10^{-14}$) and "flower development" ($p < 10^{-11}$), and all GO terms preferentially enriched at this stage were linked to cell fate specification, morphogenesis, and differentiation (Figure 1G). Accordingly, the list of high-confidence LFY targets in inflorescences included well-known developmental regulators (Table 1). For example, our studies identified the floral homeotic gene *PISTILLATA* (*PI*) as a high-confidence direct LFY target in inflorescences (Table 1 and Figure 2). Two additional genes, *SEPALLATA3* (*SEP3)*, which encodes a LFY cofactor (Liu et al., 2009b), as well as *EMBRYONIC FLOWER1* (*EMF1)*, which encodes a polycomb regulator (Calonje et al., 2008), were LFY-bound, -dependent, and -coexpressed at this stage (Figure 2A and Table 1). LFY bound to regions in the *PI* promoter previously shown to be important for proper expression of this gene (Honma and Goto, 2000). We detected strong LFY binding peaks in the promoter and in the first intron of *SEP3* (Figure 2A). A previous study showed that the *SEP3* intron is important for correct expression (de Folter et al., 2007). Finally, LFY was recruited to the 5′ UTR of *EMF1*.

To test whether LFY can indeed regulate expression of these genes, we employed a synchronous flower induction system (*ap1 cal* 35S:LFY-GR; Figure S3) (Wellmer et al., 2006). We observed rapid changes in expression of *PI*, *SEP3* and *EMF1* shortly after LFY-GR activation in *ap1 cal* inflorescences (Figure 2B). While *PI* and *SEP3* were upregulated, *EMF1* was repressed by LFY (Figure 2B). *EMF1* is a polycomb regulator thought to directly repress expression of floral homeotic genes outside of the proper developmental context (Calonje et al., 2008; Chen et al., 1997); hence, downregulation of *EMF1* expression may be a prerequisite for *AP3*, *PI,* and *AG* upregulation and flower patterning.

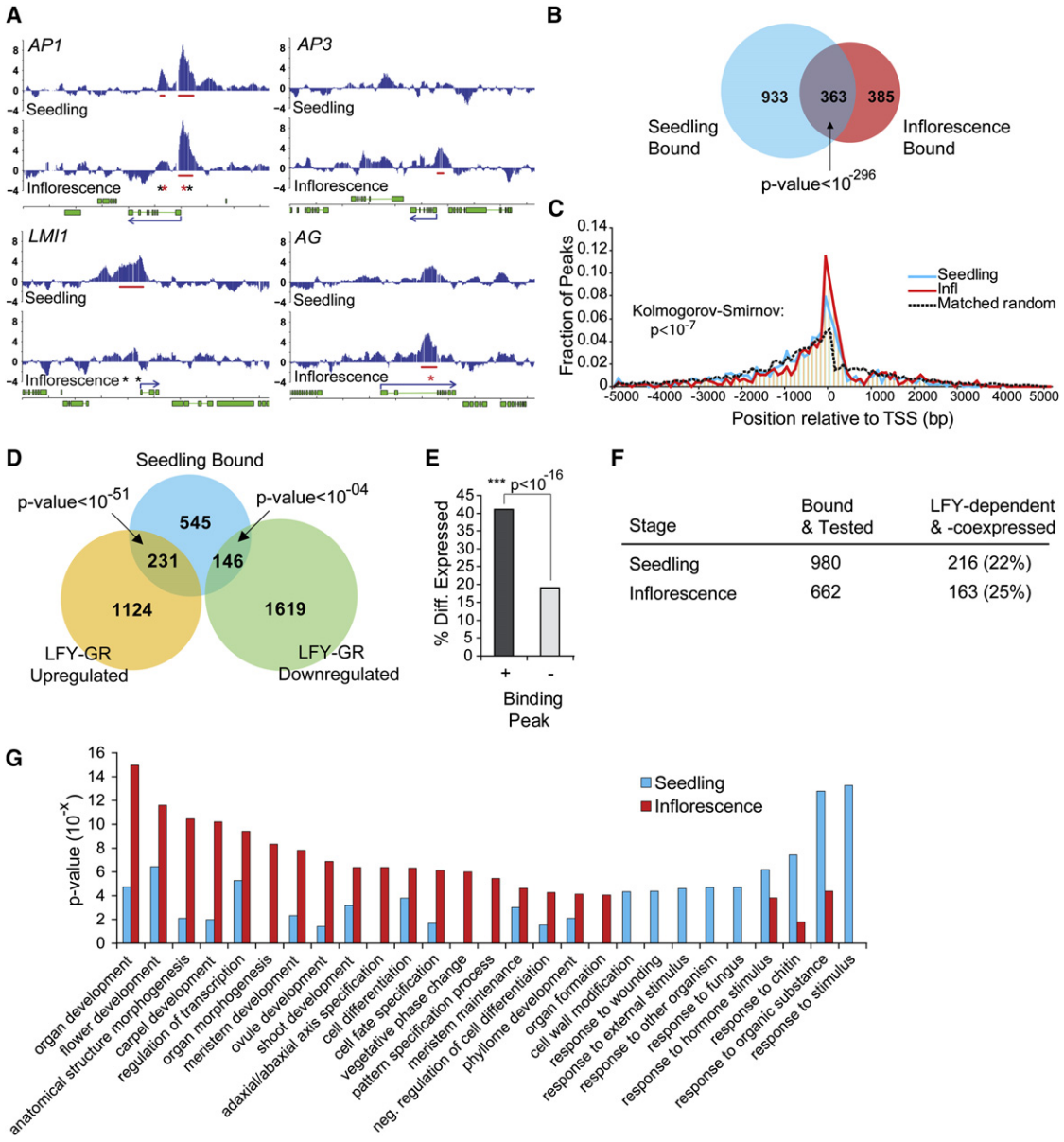


**Figure 1. Genome-Wide LFY Binding to Regulatory Regions at Two Stages in Development**

(A) Significant LFY binding at known direct LFY targets (Busch et al., 1999; Lamb et al., 2002; Wagner et al., 1999; William et al., 2004). Tracks: moving average t-statistic (20 kb window) for seedling (top) and inflorescence (bottom) ChIP-chip data. Horizontal red bars: significantly bound regions (FDR < 0.05). Asterisks: LFY consensus binding motifs in significantly bound regions ($p < 0.001$; red: primary; black: secondary; see text for details).

(B) Significant overlap (Fisher's exact test) between seedling and inflorescence LFY-bound target genes.

(C) LFY binding peaks map close to transcription start sites (TSSs). The pattern of LFY binding is significantly different from that of matched randomly generated peaks (70% intergenic, 30% genic; see Supplemental Experimental Procedures for details).

(D) Overlap of LFY-bound genes and genes differentially expressed (FDR < 0.05) in seedlings 4 hr after LFY-GR activation. Only 922 of 1296 LFY-bound genes were tested on the expression array (probe set is printed on array and passed our nonspecific filtering criteria).

(E) Presence of a seedling LFY binding peak significantly increased the probability that a gene was differentially expressed (logistic regression; $p < 10^{-16}$).

(F) Identification of high-confidence LFY-dependent and coexpressed LFY target genes (see text and Experimental Procedures for details). Nine hundred eighty seedling and 662 inflorescence targets were tested on the arrays used for the analysis.

(G) Gene ontology (GO) term enrichment ($p < 0.00005$ in at least one stage) for the high confidence LFY target genes. GO terms were grouped based on the stage of highest preferential enrichment and sorted based on p value.

See also Figures S1 and S2 and Tables S1 and S2.

The precise timing of the induction of the floral homeotic genes *AP3*, *PI*, and *AG* is central for proper flower morphogenesis; early induction leads to premature differentiation of the floral meristem, while late induction leads to the development of extra floral organs (Liu et al., 2009b). It was recently shown that this timing is critically linked to *SEP3* accumulation in the developing flower

**Table 1. Examples of High-Confidence LFY Target Genes Identified at the Inflorescence Stage**

| | AGI ID | Gene Name | Role | Stage[a] | Citation[b] |
|---|---|---|---|---|---|
| Flowering time | AT1G53160 | SPL4 (SQUA. PROMOTER BINDING PROTEIN-LIKE 4) | TXN | I | Amasino (2010); Michaels (2009) |
| | AT3G15270 | SPL5 (SQUA. PROMOTER BINDING PROTEIN-LIKE 5) | TXN | I | |
| | AT1G72830 | NF-YA8 /HAP2C | TXN | I S | |
| | AT5G47640 | NF-YB2 /HAP3B | TXN | I | |
| | AT5G60910 | FUL (FRUITFULL) | TXN | I | |
| Polarity | AT5G16560 | KAN (KANADI) | TXN | I S | Bowman and Floyd (2008) |
| | AT1G32240 | KAN2 (KANADI 2) | TXN | I | |
| | AT2G45190 | FIL (FILAMENTOUS FLOWER) | TXN | I | |
| | AT2G34710 | PHB (PHABULOSA) | TXN | I | |
| | AT2G37630 | AS1 (ASYMMETRIC LEAVES 1) | TXN | I | |
| | AT5G60450 | ARF4 (AUXIN RESPONSE FACTOR 4) | TXN | I | |
| | AT2G33860 | ETT (ETTIN) | TXN | I | |
| Floral homeotic | AT3G54340 | AP3 (APETALA 3) | TXN | I | Krizek and Fletcher (2005) |
| | AT5G20240 | PI (PISTILLATA) | TXN | I | |
| | AT4G18960 | AG (AGAMOUS) | TXN | I | |
| | AT1G24260 | SEP3 (SEPALLATA 3) | TXN | I | |
| | AT2G03710 | SEP4 (SEPALLATA 4) | TXN | I | |
| | AT5G11530 | EMF1 (EMBRYONIC FLOWER 1) | CHR | I S | |
| Flower development | AT4G37750 | ANT (AINTEGUMENTA) | TXN | I | Irish (2010); Jack (2004); van Zanten et al. (2009) |
| | AT5G10510 | AIL6 (AINTEGUMENTA-LIKE 6) | TXN | I | |
| | AT5G35770 | SAP (STERILE APETALA) | CHR | I | |
| | AT5G28640 | AN3 (ANGUSTIFOLIA 3) | CHR | I | |
| | AT3G13960 | GRF5 (GROWTH REGULATING FACTOR 5) | TXN | I | |
| | AT5G53950 | CUC2 (CUP-SHAPED COTYLEDON 2) | TXN | I | |
| | AT4G36260 | STY2 (STYLISH 2) | TXN | I | |
| | AT5G11320 | YUC4 (YUCCA 4) | BS | I | |
| | AT1G70510 | KNAT2 (KNOTTED-LIKE FROM HOMEOBOX GENE 2) | TXN | I | |
| | AT2G26330 | ER (ERECTA) | SIG | I | |
| | AT5G62230 | ERL1 (ERECTA-LIKE 1) | SIG | I S | |
| | AT5G07180 | ERL2 (ERECTA-LIKE 2) | SIG | I | |

AGI ID, locus identifier; BS, biosynthesis; CHR, chromatin-based regulation of transcription; TXN, transcription; SIG, signal transduction.
[a] Stage at which the direct LFY target gene was identified. S (seedling), I (inflorescence).
[b] Citation for functional grouping of target genes.

primordium (Kaufmann et al., 2009; Liu et al., 2009b). We therefore next investigated *SEP3* expression in *lfy* mutants compared to the wild-type using in situ hybridization and reporter studies (de Folter et al., 2007). In *lfy* mutants, we observed strongly reduced *SEP3* expression in the center of early stage 3 flower primordia (Figure 2C), the stage and tissue in which SEP3 upregulates the floral homeotic genes in wild-type plants (Liu et al., 2009b). Our data suggest that LFY directly induces the expression of its cofactor *SEP3* at this critical stage in flower development (Figure 2D).

## LFY Moderates Biotic Stress Responses

High-confidence LFY target genes at the seedling stage were significantly enriched ($p < 10^{-4}$) in GO terms linked to development (Figure 1G) and included known regulators of the switch to reproduction, as expected (Table 2). Surprisingly, the majority of the GO terms enriched at this stage were associated with plant responses to endogenous (hormone) or environmental (biotic stress) stimuli (Figure 1G). Accordingly, known hormone and biotic stimulus response pathway regulators were among the identified high-confidence LFY targets (Table 2). Modulation of hormone response gene expression by LFY is consistent with roles for these pathways in primordium initiation and flower development (Liu et al., 2009a), while identification of biotic stimulus response genes as direct LFY target genes (Table 2) suggests a role for LFY in additional survival programs. Involvement of a developmental regulator in defense responses is not unprecedented (Nurmberg et al., 2007).

Two of the defense response LFY targets we identified, the ABC transporter *PDR8*/*PEN3* and the MAMP (microbe-associated molecular pattern) recognition receptor *FLS2*, were bound and repressed by LFY (Figures 3A and 3B). Both PEN3 and FLS2 are components of a basal plant immune response pathway leading to callose deposition at the cell wall and

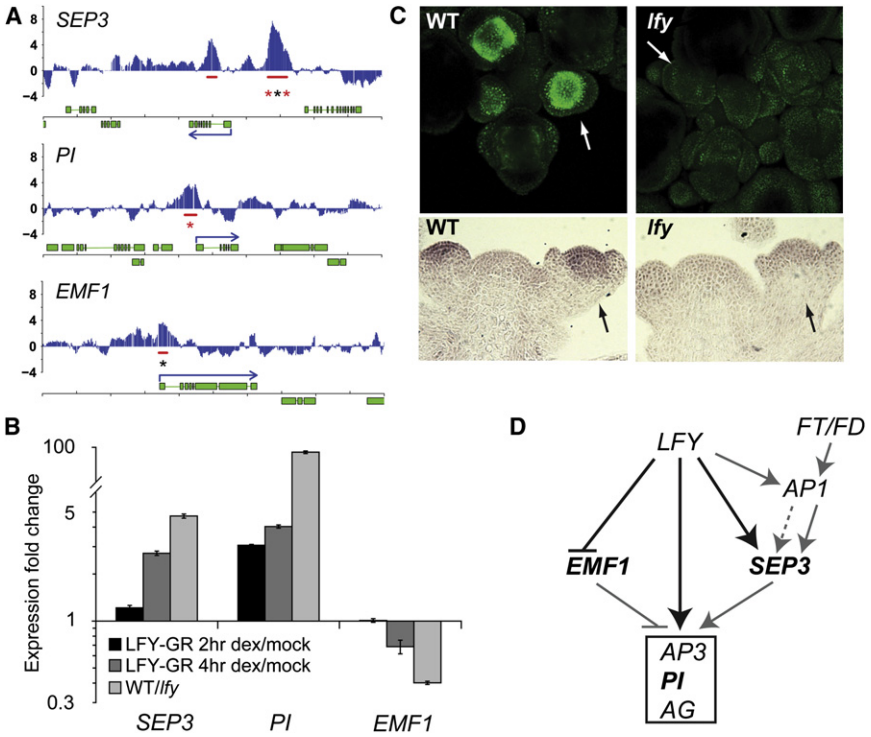


**Figure 2. LFY Directly Regulates the Expression of Well-Known Developmental Regulators**

(A) Significant LFY binding to regulatory regions of *SEP3*, *PI*, and *EMF1* in inflorescences (see Figure 1A for description of labels).

(B) Expression changes of these direct LFY targets after dexamethasone (dex) induction of LFY-GR in *ap1 cal* inflorescences relative to mock treated samples, and in wild-type (WT) compared with *lfy* null mutants in 13-day-old seedlings (*EMF1*) or in 15-day-old seedlings (*PI, SEP3*). Data shown are mean ± standard error of the mean (SEM).

(C) Top: Confocal images of wild-type and *lfy* null mutant inflorescences expressing pSEP3:SEP3-GFP (de Folter et al., 2007), which monitors LFY binding to the first intron of *SEP3*. Bottom: in situ hybridization of wild-type and *lfy* null mutant inflorescences showing expression of *SEP3*. Arrows point to young stage three flower primordia.

(D) Regulatory network controlling *AP3*, *PI*, and *AG* induction. Regulatory interactions identified here (black arrows and lettering) are supported by four independent criteria: the target gene is directly bound by LFY, coexpressed with *LFY*, and differentially expressed after LFY-GR activation and in *lfy* mutants compared with the wild-type. Dotted arrow: indirect regulation.

See Figure S3 for a comparison of LFY, AP1, and SEP3 binding data.

restriction of pathogen spread in the host (Clay et al., 2009; Zipfel et al., 2004). To investigate a possible link between LFY and this pathway, we challenged plants with a flagellin-derived peptide (flg22), which is recognized by FLS2. This yielded robust callose deposition in wild-type and in mock-treated LFY-GR seedlings, but not after prior steroid activation of LFY-GR (Figure 3C; Figures S4A and S4B).

To test for a role of endogenous LFY in this pathway, we examined callose deposits in flg22-infiltrated wild-type and *lfy* null mutant cauline leaves. *LFY* is expressed in this tissue during the meristem identity transition (Blazquez et al., 1997) (Figure S1A). We observed a significant increase in the number of flg22-induced callose deposits in *lfy* mutant relative to wild-type cauline leaves (Figure 3D). Consistent with this finding, many genes associated with this defense-induced cell wall modification pathway (Clay et al., 2009) were more highly expressed in this tissue in the *lfy* mutant than in the wild-type after flg22 treatment (Figure 3E). To probe additional FLS2-mediated downstream responses, we monitored the expression of flg22-induced defense genes not linked to callose deposition (Denoux et al., 2008). Upon flg22 stimulation, these genes also were more highly induced in *lfy* mutants than in the wild-type. Moreover, a gene encoding a lipid transfer protein inhibitor, known to be downregulated upon flg22 treatment, was more strongly repressed in *lfy* mutants (Figure 3F). Prolonged flg22 exposure inhibits plant growth (Gomez-Gomez et al., 1999). When we treated *lfy* mutant and wild-type seedlings for eight days with flg22 immediately after the meristem identity transition (in 11-day-old seedlings; Blazquez et al., 1997), the *lfy* seedlings exhibited more dramatic growth defects than the wild-type (Figure 3G). No significant difference in growth was observed between wild-type and *lfy* mutant seedlings when the treatment was initiated in younger seedlings (5-day-old; data not shown). Finally, we examined growth of a virulent bacterial strain (*Pseudomonas syringae* pv. *tomato* (*Pst*) DC3000) on wild-type and *lfy* mutant cauline and adult (late arising) rosette leaves; *LFY* is known to be expressed in the primordia of these leaves (Figure S1) (Blazquez et al., 1997). We observed a modest but significant decrease (3.5-fold, $p < 0.01$) in bacterial growth in the *lfy* mutant compared with the wild-type (Figure 3H; Figures S4C and S4D). Also, *lfy* mutant cauline leaves developed noticeably fewer disease symptoms than those of the wild-type (Figure 3H). These visible differences were not observed in *lfy* mutant rosette leaves (data not shown), consistent with the higher level of *LFY* expression in the later arising cauline leaf primordia (Blazquez et al., 1997). Wild-type and *lfy* mutant rosette leaves from 4-week-old short-day grown plants did not display differential defense gene expression, callose deposition, or pathogen growth when challenged with *Pst* DC3000 (Figures S4E–S4H), consistent with these leaves having formed prior to *LFY* induction (Blazquez et al., 1997; Hempel et al., 1997). Taken together, our results point to a role for LFY in reducing defense responses triggered by the MAMP flg22 and by bacterial pathogen challenge that may in part be attributable to downregulation of *FLS2* and *PEN3* levels by LFY.

## De Novo Identification of Potential LFY Binding and Cofactor Motifs

The currently known LFY consensus binding motif, CCANTG[G/T], is based on only two experimentally confirmed LFY target genes (Busch et al., 1999). To better define a consensus LFY binding motif, we queried a subset of the seedling-and-inflorescence-bound

**Table 2. Examples of High-Confidence LFY Target Genes Identified at the Seedling Stage**

| | AGI ID | Gene Name | Role | Stage[a] | Rapid DE[b] | Citation[c] |
|---|---|---|---|---|---|---|
| Flowering time | AT4G35900 | FD | TXN | S | x | Amasino (2010); Michaels (2009); Yant et al. (2009) |
| | AT2G17770 | FDP (FD PARALOG) | TXN | S I | | |
| | AT1G27360 | SPL11 (SQUA. PROMOTER BINDING PROTEIN-LIKE 11) | TXN | S | | |
| | AT5G67180 | TOE3 (TARGET OF EAT1 3) | TXN | S | x | |
| | AT1G25560 | TEM1 (TEMPRANILLO 1) | TXN | S I | x | |
| Meristem identity | AT5G61850 | LFY (LEAFY) | TXN | S I | NA | Albani and Coupland (2010); William et al. (2004) |
| | AT1G69120 | AP1 (APETALA1) | TXN | S I | x | |
| | AT1G16070 | AtTLP8/LMI5 (LATE MERISTEM IDENTITY 5) | SIG | S I | x | |
| | AT3G61250 | MYB17/LMI2 (LATE MERISTEM IDENTITY 2) | TXN | S I | x | |
| | AT5G03840 | TFL1 (TERMINAL FLOWER 1) | SIG | S I[d] | x | |
| Hormone response | AT2G34650 | PID (PINOID) | T | S I | x | Bowman and Floyd (2008); Guilfoyle and Hagen (2007); Liu et al. (2009a) |
| | AT4G31820 | ENP (ENHANCER OF PINOID); NPY1 | T | S | x | |
| | AT5G67440 | NPY3 | T | S | | |
| | AT2G01420 | PIN4 (PIN-FORMED 4) | T | S | | |
| | AT3G23050 | IAA7 (AUXIN RESISTANT 2) | TXN | S | | |
| | AT1G04250 | AXR3 (AUXIN RESISTANT 3); IAA17 | TXN | S I | x | |
| | AT2G33860 | ETT (ETTIN); ARF3 | TXN | S I | | |
| | AT5G56300 | GAMT2 (GIBBERELLIC ACID METHYLTRANSFERASE 2) | BS | S | | Mutasa-Gottgens and Hedden (2009) |
| | AT3G63010 | GID1B (GA INSENSITIVE DWARF1B) | RE | S | x | |
| Biotic stimulus response | AT2G39660 | BIK1 (BOTRYTIS-INDUCED KINASE 1) | SIG | S | | Burow et al. (2010); Clay et al. (2009); Dodds and Rathjen (2010) |
| | AT5G46330 | FLS2 (FLAGELLIN-SENSITIVE 2) | SIG | S | x | |
| | AT1G59870 | PDR8/PEN3 (PLEIOTROPIC DRUG RESISTANCE 8) | T | S | | |
| | AT5G61420 | MYB28 (MYB DOMAIN PROTEIN 28) | TXN | S | x | |
| | AT1G32540 | LOL1 (LSD ONE LIKE 1) | TXN | S | x | |
| | AT2G38470 | WRKY33 (WRKY DNA-BINDING PROTEIN 33) | TXN | S | x | |
| | AT1G80840 | WRKY40 (WRKY DNA-BINDING PROTEIN 40) | TXN | S I | | |
| | AT4G31800 | WRKY18 (WRKY DNA-BINDING PROTEIN 18) | TXN | S | x | |
| | AT5G49520 | WRKY48 (WRKY DNA-BINDING PROTEIN 48) | TXN | S I | x | |

AGI ID, locus identifier; BS, biosynthesis; RE, receptor; SIG, signal transduction; T, transport; TXN, transcription.
[a] Stage at which the direct LFY target gene was identified. S (seedling), I (inflorescence).
[b] Genes significantly differentially expressed (FDR < 0.05) after 4 hr steroid activation of LFY-GR (expression array, see methods).
[c] Citation for functional grouping of target genes.
[d] LFY bound site in the 3′ intergenic region.

regions with a novel sequential analysis pipeline, which utilizes predictions from five popular motif-finding algorithms (see methods for details). We identified a 19 bp palindromic presumptive LFY binding motif, henceforth termed the "primary" LFY motif, that was strongly enriched ($p < 10^{-145}$) in all LFY-bound regions (Figure 4A; Figures S5A and S5B). A single motif prediction algorithm (Bailey and Elkan, 1995) identified a similar motif (Figure S5C). This primary LFY motif contained critical nucleotides contacted by a LFY DNA binding domain homodimer based on protein/DNA cocrystals (Hames et al., 2008) (Figure 4A). The previously identified CCANTG[G/T] consensus, while contained within the primary binding motif, was itself only marginally enriched (Figure 4A).

Many of the observed significant LFY binding events were specific to the seedling or the inflorescence data set (Figure 1B). For example, the known meristem identity regulator *LMI1* was bound by LFY only at the seedling stage, while the floral homeotic genes *AP3* and *AG* were bound only at the inflorescence stage (Figure 1A). To test for LFY binding motif variants that may contribute to this stage-specific LFY recruitment, we repeated our de novo motif analyses for a subset of regions bound only in inflorescences or only in seedlings. In inflorescences, we identified a motif similar to the primary LFY consensus motif (Figure S5A). Importantly, our analysis of seedling-only bound regions revealed a potential secondary LFY consensus motif, which was highly enriched in LFY-bound regions identified at the seedling stage ($p < 10^{-45}$) (Figures 4B and 4C; Figures S5A and S5B). This motif mainly differs from the primary LFY consensus at the +2 position relative to the motif core with a thymine preferred to guanine. A similar secondary

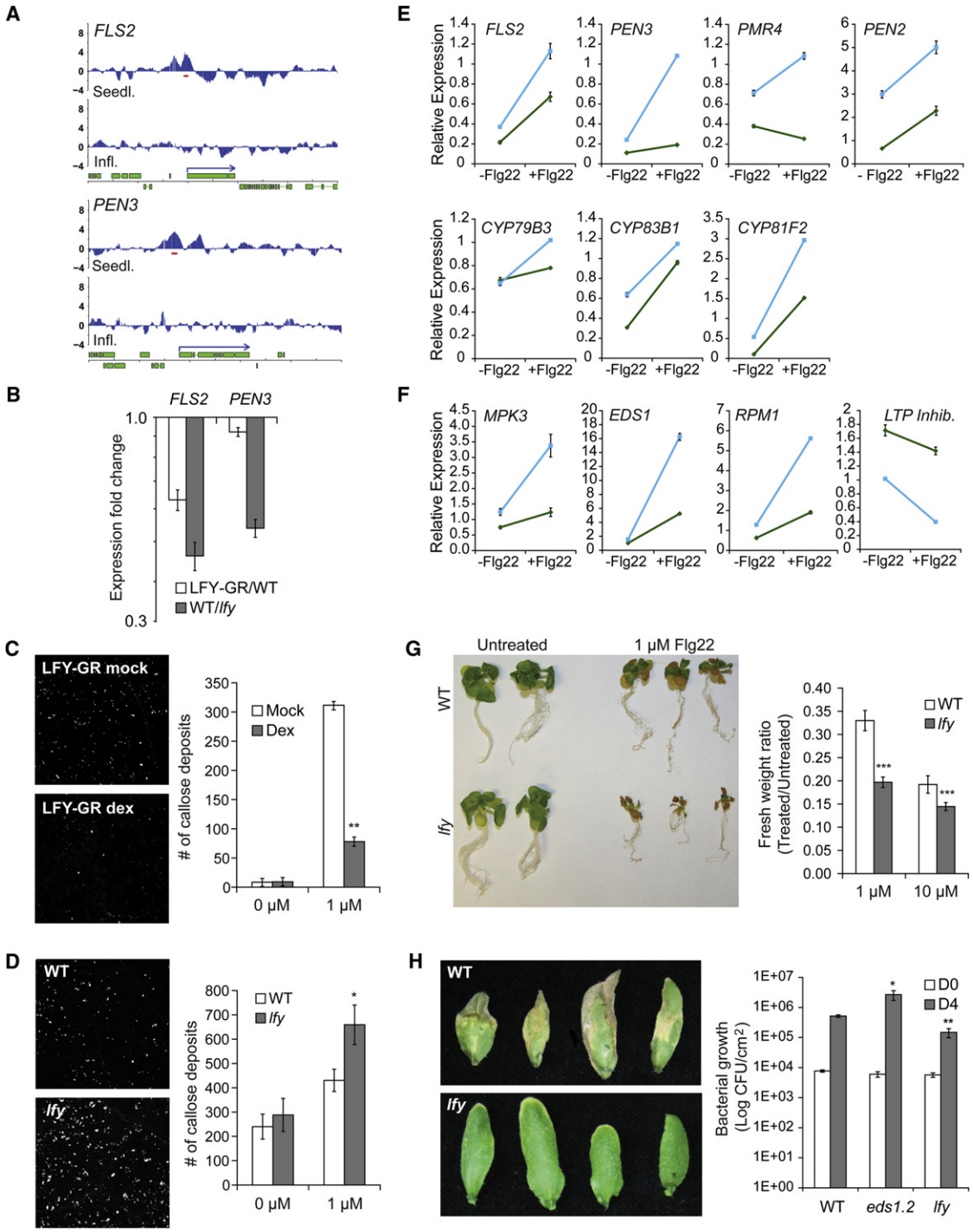


**Figure 3. LFY Represses Responses to the Bacterial Flagellin Peptide flg22 and Pathogen Challenge**

(A) Significant LFY binding to regulatory regions of *FLS2* and *PEN3* in seedlings (see Figure 1A for description of labels).

(B) Expression changes observed for *FLS2* and *PEN3* in wild-type (WT) and *lfy* mutant cauline leaves or after dexamethasone treatment of LFY-GR and wild-type seedlings. Seedling expression is based on our transcriptome analysis.

(C and D) Callose deposition triggered by flg22 in dexamethasone (dex) versus mock treated LFY-GR seedlings (C) and in *lfy* null mutant compared to wild-type cauline leaves (D). Right: quantification of callose foci from two independent experiments.

(E and F) Expression of direct LFY targets (*FLS2*, *PEN3*, *CYP79B3*, and *CYP83B1*) and other defense genes 1 hr after mock (-flg22) or flg22 infiltration of *lfy* (blue line) and wild-type (green line) cauline leaves. (E) Genes linked to flg22-induced callose deposition (Clay et al., 2009). (F) Flg22-regulated defense genes not linked to callose deposition.

(G) Growth suppression by flg22 in *lfy* mutant compared to wild-type seedlings. Right: Quantification of biomass. Left: Photograph after 8 days of treatment.

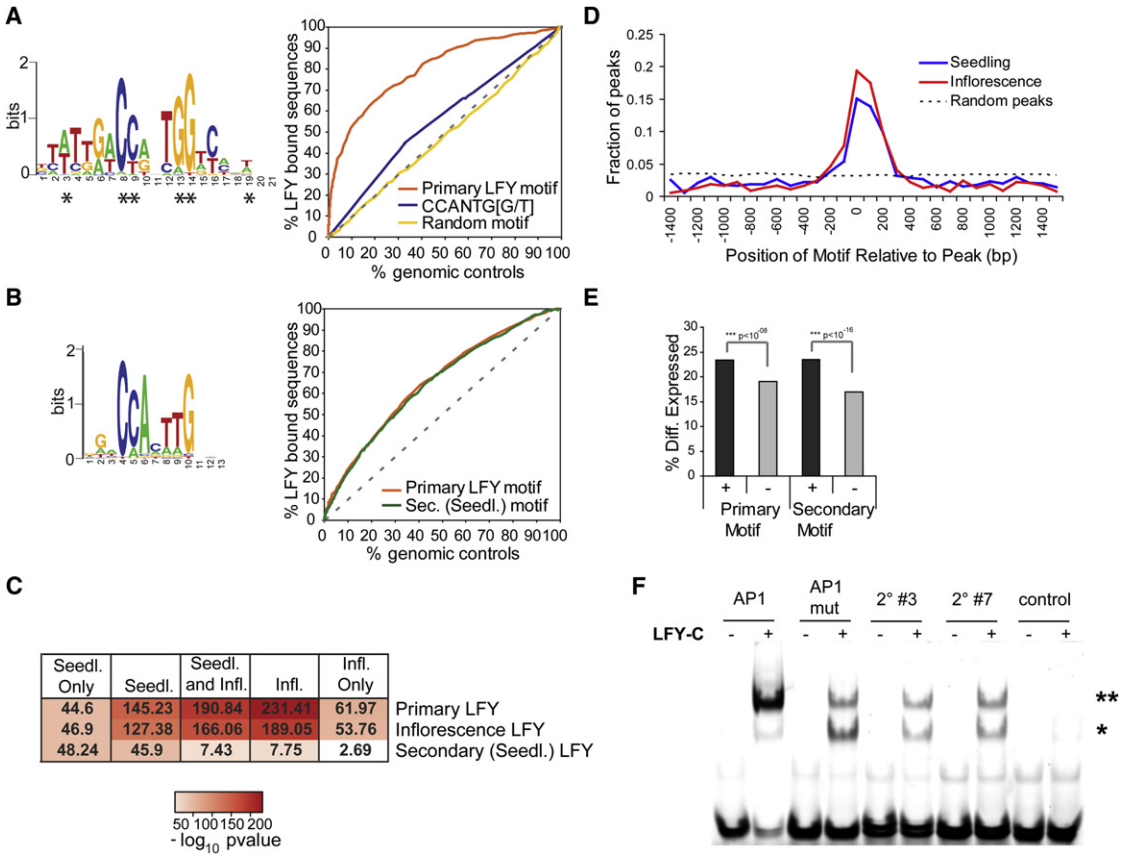


**Figure 4. LFY Consensus Binding Motifs**

(A) Left: primary LFY consensus motif identified by sequential motif analysis from a subset of the seedling-and-inflorescence bound regions. Asterisks: Nucleotides contacted by the LFY protein in LFY/DNA cocrystals (Hames et al., 2008). Right: Enrichment of the primary LFY motif, the previously known CCANTG[G/T] consensus (Busch et al., 1999), and a randomly permuted primary motif in all seedling-and-inflorescence bound regions based on receiver operating characteristic (ROC) curve analysis.

(B) Left: secondary LFY binding motif identified by sequential motif analysis from a subset of the seedling-only bound regions. Right: ROC curve analysis of both LFY motifs in all seedling-only bound sequences.

(C) Enrichment ($-\log_{10}$ p values) of de novo identified LFY motifs. Enrichment was tested in sequences bound by LFY in seedlings (Seedl.), in inflorescences (Infl.), at both stages (Seedl. and Infl.), in seedlings but not inflorescences (Seedl. Only) and in inflorescences but not seedlings (Infl. Only).

(D) Locations of the highest-scoring primary LFY motif within the 3000 bp surrounding LFY binding peak maxima (red and blue lines) or within 3000 bp of randomly generated peak maxima (dotted line).

(E) Presence of primary or secondary (seedling) LFY consensus motifs significantly enhances the probability of differential gene expression after LFY activation (logistic regression).

(F) Gel shift to test LFY binding to a primary motif (*AP1*), to an *AP1* motif containing only one LFY binding site (*AP1m*), to the secondary motif #3 (AT1G66480) and #7 (AT3G21890), and to an unrelated negative control motif. (**) dimeric LFY binding; (*) monomeric LFY binding.

See also Figure S5 and Table S3.

motif was identified when using a single motif prediction algorithm (Bailey and Elkan, 1995) (Figure S5C).

Both the primary and secondary motifs mapped close to the center of LFY binding peaks (Figure 4D; Figure S5D) and were present at regulatory regions of many known LFY target genes, as well as those identified here (Figures 1A and 2A; Figure S1E). Furthermore, the two LFY motifs together explain the majority of the LFY peaks observed (>72%; Table S3). Finally, the presence of a presumptive primary or secondary LFY motif near a given locus significantly enhanced the probability that it will be differentially expressed in response to LFY activation ($p < 10^{-08}$, logistic regression; Figure 4E).

(H) Right: Bacterial growth on adult rosette and cauline leaf discs of long-day grown plants after infection with *Pseudomonas syringae* pv. *tomato (Pst)* DC3000 measured at 0 and 4 days after inoculation. The L*er eds1.2* mutant which exhibits enhanced susceptibility to bacterial pathogens was used as an infection control (Feys et al., 2005). Left: infiltrated cauline leaves at day 4.

(B and D–H): Data shown are mean ± SEM. Asterisks: Student's t test $p < 0.05$ (*), $< 0.005$ (**), $< 0.0005$(***). The same trend was observed in two independent experiments.

See also Figure S4.

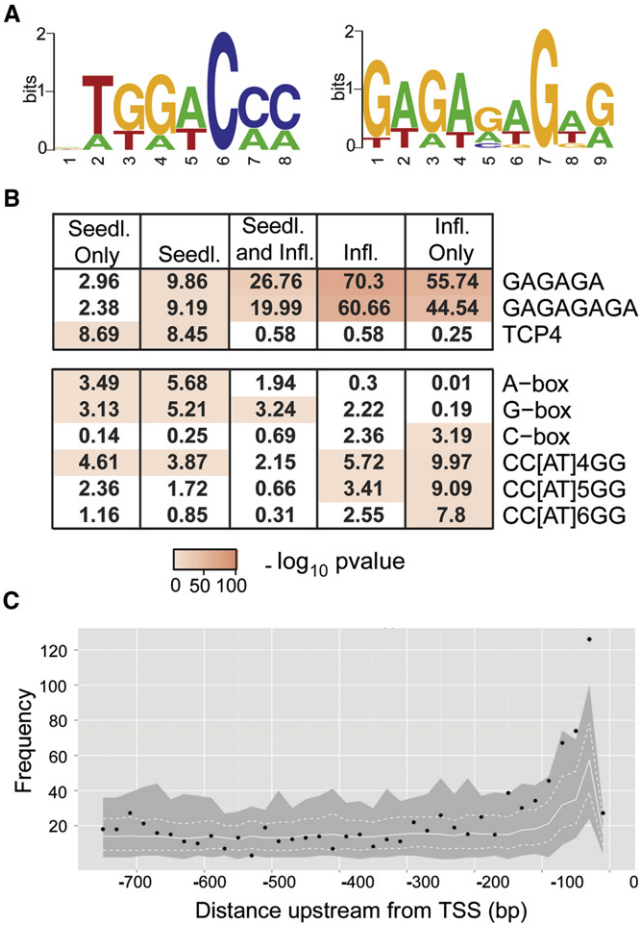


**Figure 5. Identification of Potential LFY Cofactor Motifs**

(A) De novo motif analysis of LFY-bound regions identified a motif with similarity to a class II TCP transcription factor binding motif (left), and a GA-rich motif (right).

(B) (Top) Enrichment ($-\log_{10}$ p values) of these cofactor motifs in LFY-bound regions. (Bottom) Enrichment of motifs of known LFY cofactors: bZIP (A-,G-, and C-boxes) and MADS $(CC[AT]_{4\text{-}6}GG)$ (Krizek and Fletcher, 2005). No enrichment for homeodomain transcription factor binding sites was observed. Stages and categories are as described in Figure 4C.

(C) Black dots: Positional frequencies of GAGAGA repeats for LFY bound promoters in inflorescences. Gray ribbon: GAGAGA frequencies in TAIR9 promoters, with a solid white line indicating the mean and dashed lines indicating the 5th and 95th percentiles. The spike in GA-repeats at −35 bp from the TSS (position 0) in the genomic background shows an underlying tendency toward GA-rich sequences in core promoters of many *Arabidopsis* genes (Yamamoto et al., 2009).

To test whether the secondary motif can recruit LFY, we performed electrophoretic mobility shift assays (EMSAs) as well as yeast one-hybrid binding studies. The palindromic LFY binding site in *AP1* served as a representative primary motif (this study; Hames et al., 2008). The C-terminal DNA binding domain of LFY (LFY-C) bound to all seven tested secondary motifs based on EMSAs (Figure 4F; Figure S5E). The affinity of LFY-C for the secondary motifs was much lower than for the primary motif but comparable to that of an *AP1* motif in which one of the two LFY-bound half-sites (Hames et al., 2008) was mutated (Figure 4F; Figure S5E). In addition, LFY fused to the strong VP16 activation domain was able to confer increased growth of yeast to the fungal inhibitor aureobasidin A when recruited to a secondary motif, while LFY alone was not (Figure S5F), in agreement with prior studies which showed that LFY alone is not sufficient to activate transcription in the yeast one-hybrid assay (Parcy et al., 1998).

The de novo motif analysis also identified two potential LFY cofactor motifs, most notably a TGG(A/T)CC(C/A) motif and a GA-rich motif (Figure 5). The former is similar to the TCP4 transcription factor binding motif (Schommer et al., 2008). The TCP4 motif was significantly enriched in seedling-bound regions, while GA-repeat hexamer and octamer motifs were highly significantly enriched in inflorescence-bound regions (Figures 5B and 5C), suggesting that these elements may recruit stage-specific LFY cofactors. We also assessed the enrichment of known LFY cofactors (Figure 5B).

GA-repeat motifs are often found in Polycomb Responsive Elements (PREs) (Schuettengruber and Cavalli, 2009); hence, inflorescence-stage LFY targets may perhaps be repressed by polycomb group proteins at other developmental stages. Consistent with this hypothesis, the LFY inflorescence targets *AP3*, *AG*, and *SEP3* are regulated by polycomb repression (Goodrich et al., 1997; Liu et al., 2009b). In addition, our high-confidence inflorescence LFY target gene list was significantly enriched ($p < 0.05$) in genes repressed by polycomb-group proteins in seedlings (Table S4) based on queries of publicly available data sets (Oh et al., 2008; Turck et al., 2007) (http://affymetrix.arabidopsis.info/narrays/RefSearch.pl?ref_number=425).

## DISCUSSION

Here, we present a genome-wide identification of direct LFY target genes. Many of the genes we identified are also bound by the known LFY cofactors SEP3 and AP1 (see http://published.genomics.upenn.edu/2010/LEAFY) (Irish, 2010; Liu et al., 2009b), in further support of their physiological relevance.

The three floral homeotic genes *AP3*, *AG*, and *PI* specify the identity of the reproductive organs of the flower, the stamens and carpels (Krizek and Fletcher, 2005). Regulation of the expression of these genes is, therefore, critical for reproductive success. Prior studies had revealed a direct role for LFY in induction of *AP3* and *AG* (Busch et al., 1999; Lamb et al., 2002). We show that LFY, in addition, directly upregulates the floral homeotic gene *PI*, in agreement with the previous demonstration that *PI* expression in developing flowers is strongly dependent on LFY (Weigel and Meyerowitz, 1993). We further report that LFY directly represses the polycomb group protein *EMF1* that prevents precocious activation of the floral homeotic genes (Calonje et al., 2008). In support of this, *emf1* null mutants are epistatic to *lfy* null mutants and LFY overexpression enhances a weak but not a null *emf1* mutant (Chen et al., 1997). Downregulation of *EMF1* by LFY may be required to overcome chromatin repression for initiation of flower patterning.

Finally, we show that LFY directly activates *SEP3* expression in the center of young flower primordia. LFY and SEP3 together induce *AP3*, *PI* and *AG* (Liu et al., 2009b). Thus, as reported for other developmental master regulators (for example, see

Tapscott, 2005), LFY activates expression of its own cofactor. The direct LFY target AP1 (Parcy et al., 1998; Wagner et al., 1999) also induces *SEP3* (Kaufmann et al., 2010; Liu et al., 2009b). *AP1* expression in flower primordia is redundantly activated by LFY, and by additional pathways such as the photoperiod flowering time pathway via FT and FD (Ruiz-Garcia et al., 1997; Wagner et al., 1999; Liu et al., 2009a). Hence, parallel converging pathways control *SEP3* induction (Figure 2D).

Our study, combined with previous findings (Calonje et al., 2008; Kaufmann et al., 2009, 2010; Liu et al., 2009b; Wagner et al., 1999), suggests that LFY operates as a highly connected regulatory 'hub' (Luscombe et al., 2004) upstream of three interlocking feed-forward loops that control the upregulation of *AP3*, *PI*, and *AG* expression. Such feed-forward loops function as signal persistence indicators and delay elements (Alon, 2007). In the context of floral homeotic gene regulation, the network that we describe would constrain upregulation of the floral homeotic genes to cells with robust accumulation of both LFY and SEP3, and ensure a delay in the induction of these genes relative to the time of floral initiation, preventing precocious differentiation and termination of the floral meristem.

How transcription factors regulate different target genes in different cell types and developmental stages is not well understood (Farnham, 2009). Our study uncovered two possible mechanisms that deserve further evaluation: selective LFY recruitment (by stage-specific *cis* and trans factors) and selective chromatin constraints (polycomb repression). Based on protein-binding microarrays, 50% of the transcription factors assayed recognize both a primary and a secondary consensus motif (Badis et al., 2009). We defined a palindromic primary LFY and a secondary (seedling) LFY consensus motif. LFY is predicted to bind the palindromic motif as a homodimer (Hames et al., 2008). LFY bound to the secondary motif in vitro; however the binding affinity is likely too low for the motif alone to recruit LFY in vivo, in particular at the seedling stage when less LFY protein is present. This finding, combined with the nonpalindromic nature of the secondary motif, suggests that LFY recruitment at the seedling stage may involve a second transcription factor. This factor might assist in recruitment by interacting with a nearby sequence and forming a heterodimeric complex with a LFY monomer (see Hollenhorst et al., 2009) or, alternatively, by modifying the affinity of the LFY homodimer for the secondary binding motif. Consistent with these ideas, LFY physically interacts with at least one other transcription factor (Liu et al., 2009b). The two LFY consensus motifs together explain the majority of the LFY binding peaks. The remaining binding events may be due to the presence of additional LFY motifs or, alternatively, to "piggybacking" of LFY to some regulatory regions by direct interaction with another transcription factor (Farnham, 2009).

We further identified motifs for potential LFY cofactors. Particularly intriguing among these were GAGA motifs preferentially enriched in LFY-bound sequences in inflorescences. This raises the possibility that, as in *Drosophila* and mammals (Schuettengruber and Cavalli, 2009; Sing et al., 2009), GAGA motifs may play a role in recruitment of polycomb group proteins in plants. Indeed, the high-confidence inflorescence LFY targets are enriched for genes whose expression is repressed by polycomb group proteins prior to flower formation. The identified direct repression of the polycomb regulator *EMF1* by LFY further suggests that LFY may play an active role in altering these chromatin constraints during flower patterning.

Developmental changes in resistance to pathogens and pests have been observed in many plant species (Develey-Riviere and Galiana, 2007; Herms and Mattson, 1992). Activation of defense responses can incur substantial fitness costs in terms of growth and reproduction (Heil, 2002; Tian et al., 2003). We report here that LFY modulates the plant immune response to pathogens. We show that LFY is required to repress plant responses to the bacterial MAMP flg22 and to reduce resistance to bacterial colonization and disease symptoms in leaves that form during the meristem identity transition. The data suggest that at this critical juncture in plant development LFY directs plant resources away from defense responses in these tissues and toward flower and fruit development in order to maximize reproductive fitness.

It remains to be seen whether a role for LFY in immune response is limited, for example, to plants with monocarpic life strategies like *Arabidopsis*, or observed more broadly. LFY orthologs have been identified in all species of land plants investigated, including nonflowering species (Moyroud et al., 2010). Our analysis of a public transcriptome data set (Maizel et al., 2005) revealed that LFY orthologs from additional flowering and nonflowering plant species also regulate target genes linked to plant defense (Figure S6). It is tempting to speculate that regulation of defense responses may be an ancestral LFY role; however, thus far there is no direct evidence for this conjecture and little is known about the molecular mechanisms underlying pathogen defense outside of seed plants.

Tradeoffs between stress avoidance and resource allocation to growth and reproduction are important for plant fitness and crop yield (Heil, 2002; Roux et al., 2006; Tian et al., 2003). Our studies suggest a possible mechanism for the coordination of developmental phase and defense programs. This finding is of potential ecological and also agricultural significance, given that many plant species of agricultural import including domesticated grains and many vegetable crops have monocarpic life strategies. A role for LFY in plant immune response may have gone unnoticed because pathogen response experiments are routinely performed on short-day grown plants that do not yet express *LFY*. It will be interesting to examine whether LFY links the onset of reproduction with additional, as yet undiscovered, stress responses.

## EXPERIMENTAL PROCEDURES

### Plant Materials and Growth Conditions

Plants of the Landsberg *erecta* (L*er*) accession were used. 35S:LFY-GR, *lfy-6* 35S:LFY-GR, and SEP3:SEP3-GFP were described previously (de Folter et al., 2007; Wagner et al., 1999). *ap1-1 cal-1* 35S:LFY-GR was a generous gift from Frank Wellmer. Because *lfy* mutants are sterile (Weigel et al., 1992), we obtained homozygous *lfy* null mutant seed by treating the parental *lfy-6* 35S:LFY-GR line with dexamethasone. Seeds cold-treated for 7 days at 4°C were grown in inductive conditions (continuous light or 16 hr long-day light conditions) or noninductive conditions (10 hr short-day light conditions) at 23°C at a fluence rate of 45 μmol/$m^2$ sec on 0.5× Murashige and Skoog plates (seedling experiments), or in soil (all other experiments).

### RNA Analyses

Shoot apices from 9-day-old 35S:LFY-GR and L*er* seedlings were treated with 10 μM dexamethasone in 0.1% ethanol, for 4 hr as described (Wagner et al., 1999). RNA was extracted from four independent pools of apices using TRI-Reagent, column purified (RNeasy kit; QIAGEN), and amplified and labeled using NuGEN's Ovation RNA kits. Hybridization to the Affymetrix *Arabidopsis* ATH1 array was performed at the University of Pennsylvania Microarray Core Facility. Microarray data were processed using Bioconductor packages in R. Data were gcRMA normalized (Wu et al., 2004). Nonspecific filtering was performed with the MAS5.0 algorithm for genes that were "present" in at least two of four arrays in at least one treatment group (McClintick and Edenberg, 2006). Differentially expressed genes were identified using LIMMA (Smyth, 2004). For overlap analyses between LFY-bound genes and expression array data, only bound genes tested on the array were included, i.e., a probe set for the gene was printed on the array and passed our nonspecific filtering criteria.

For expression analysis of developmental regulators, 23-day-old long-day grown *ap1-1 cal-1* 35S:LFY-GR inflorescences were dipped for 1 min in a solution containing, 0.015% silwet77 and 0.01% ethanol alone or with 1 μM dexamethasone. RNA was isolated 2, 4, and 8 hr after treatment for dexamethasone-treated, and after 8 hr for mock-treated plants. For analysis of defense gene expression, the two basal-most fully expanded cauline leaves (long-day experiments) or fully expanded rosette leaves (short-day experiments) of L*er* and *lfy* null mutant plants were infiltrated with either 10 μM flg22 or water as previously described (Kim and Mackey, 2008). Leaves were harvested 1 and 3 hr after treatment. RNA isolation and cDNA synthesis were as described in (Yamaguchi et al., 2009). For all real-time PCR analyses the mean and standard error were determined using three technical replicates; one representative experiment is shown. Primers are listed in the Supplemental Experimental Procedures. In situ hybridization was performed as in (Yamaguchi et al., 2009) using probes previously described (Liu et al., 2009b).

### ChIP-Chip Experiments

Chromatin immunoprecipitation (ChIP) was performed using 9-day-old seedlings treated with 10 μM dexamethasone, 0.1% ethanol, for 4 hr or 19-day-old untreated inflorescences with an anti-LFY antibody (Wagner et al., 1999) as described (Kwon et al., 2005) except that DNA was sonicated to an average size range of 300–500 bp.

ChIP and input DNA were amplified (see Supplemental Experimental Procedures) and hybridized to Affymetrix *Arabidopsis* 1.0R whole-genome tiling arrays. Three biological replicate 35S:LFY-GR IP samples and the corresponding input samples were hybridized for the seedling experiment while five biological replicate L*er* IP samples and the corresponding input samples were hybridized for the inflorescence experiment. The increased number of replicates enhanced peak detection for ChIP of endogenous LFY. Raw data were quantile normalized and significant binding regions were detected in CisGenome (Ji et al., 2008), employing the moving average method with a window size of 300 bp. Significant LFY binding peaks were assigned to genes using a custom Python script (see Supplemental Experimental Procedures for details).

### Identification of High-Confidence LFY-Dependent and Coexpressed Genes

LFY-dependent genes were selected based on a statistically significant change in gene expression in *lfy* mutant relative to wild-type plants using LIMMA (FDR <0.05 and |fold change| >1.5; Smyth, 2004). Coexpressed genes were defined as those with expression patterns significantly correlated or anti-correlated with *LFY* or with the direct LFY targets *AP1*, *AP3*, or *AG* (bait genes). Known LFY target genes were included in the correlation analysis since target genes often exhibit a delay in gene expression relative to the transcription factor that regulates them (Chang et al., 2005). We used a Pearson's p value cutoff (<0.05) for the correlation analysis, which corresponds to an FDR of less than 0.15. See Supplemental Experimental Procedures for details regarding the expression data sets employed.

### GO Term Analysis

Significant GO terms were identified using the GOstats Bioconductor package in R. Only GO terms annotated to more than ten genes were included. A combination of automated and manual curation was used to reduce redundancy of significant GO terms. Terms containing genes that overlapped by more than two-thirds were flagged and the more specific term was retained. In a few cases, the general term was deemed more informative and was retained instead.

### De Novo Motif Prediction

Sequence regions of 500 and 750 base pairs surrounding the LFY peaks were used to generate sequence sets bound by LFY in (1) both seedlings and inflorescences, (2) seedlings but not inflorescences (seedling only), and (3) inflorescences but not seedlings (inflorescence only). For each sequence set and sequence length, three collections of 30 randomly pulled sequences from the top 50 most significantly LFY-bound sequences (FDR <0.01) were generated. The resulting 18 data sets were fed to a prediction pipeline consisting of five well cited prediction programs: MEME, AlignAce, MotifSampler, BioProspector, and Weeder (Bailey and Elkan, 1995; Hughes et al., 2000; Liu et al., 2001; Pavesi et al., 2001; Thijs et al., 2001). The most significantly enriched motifs from each of the five programs were aligned using a sliding window analysis for the shortest average Euclidean distance and merged additively, resulting in the primary, secondary (seedling only), and inflorescence only motifs. See Supplemental Experimental Procedures for further details.

### Electrophoretic Mobility Shift Assay

The C-terminal DNA binding domain of LFY (LFY-C) was purified as described (Hames et al., 2008). For EMSAs, Cy5-dCTP labeled (GE Healthcare) oligos were used (see Supplemental Experimental Procedures). Binding reactions were performed in 20 μl binding buffer supplemented with 28 ng/μl fish sperm DNA (Roche), using 10 nM double-stranded DNA probe and 1 or 3 μM LFY-C. Binding reactions were loaded onto native 8% polyacrylamide gels and electrophoresed in 0.5 × TBE at 4°C. Gels were scanned on a Typhoon 9400 scanner.

### Flg22 Treatment and Callose Staining

For seedling callose assays, 35S:LFY-GR and wild-type were grown for 9 days in long-day conditions in liquid culture essentially as previously described (Clay et al., 2009). Dexamethasone (10 μM) in 0.1% ethanol or 0.1% ethanol alone was added to the media, followed by 1 μM flg22 peptide (GenScript Corp, Piscataway, NJ) or water application 4 hr later. Plants were fixed after approximately 20 hr, washed, and stained with aniline blue as previously described (Clay et al., 2009). For leaf assays, plants were grown and infiltrated as for RNA analyses, except 1 μM flg22 was used. Leaves were fixed after 8 hr, washed, stained, and visualized as described above. Callose deposits were visualized on a Zeiss Axiovert microscope using UV illumination and a DAPI filter set. For growth inhibition in response to flg22, wild-type and *lfy* null mutant seedlings were treated as described (Gomez-Gomez et al., 1999). After 7 days of growth in long-day conditions seedlings were transferred to liquid culture. On day 11 seedlings were treated with 1 or 10 μM flg22 and photographed and weighed 8 days later.

### Bacterial Growth Assays

*Pseudomonas syringae* pv. *tomato* (*Pst*) strain DC3000 was grown for 24 hr at 28°C on NYGA solid medium supplemented with 100 μg/mL rifampicin. Bolting plants (long-day experiments) or 4-week-old rosette leaves (short-day experiments) were spray-inoculated with bacterial suspensions at 4 × $10^8$ cfu/ml in 10 mM $MgCl_2$ with 0.04% (v/v) Silwet L-77. In planta bacterial titers were determined 3 hr (day 0) and 4 days postinoculation by shaking leaf discs in 10 mM $MgCl_2$ with 0.01% (v/v) Silwet L-77 at 28°C for 1 hr as described previously (García et al., 2010; Tornero and Dangl, 2001; Vlot et al., 2008). Dilutions of the resulting bacterial suspension were then plated on NYGA solid medium containing rifampicin and grown at 28°C prior to colony counting. Titers were measured as the mean of four replicates (day 0) or six replicates (day 4), with each replicate containing three or more leaf discs. Bacterial numbers were compared between lines using a two-tailed Student's t test. The L*er eds1.2* mutant which exhibits enhanced susceptibility to *Pst* DC3000 (Feys et al., 2005) was used as an infection control.

## ACCESSION NUMBERS

The raw data are deposited in NCBI's Gene Expression Omnibus and are accessible through the GEO Super Series accession number GSE28063. Processed data are available at our genome browser (http://published.genomics.upenn.edu/2010/LEAFY).

## SUPPLEMENTAL INFORMATION

Supplemental Information includes six figures, four tables, and Supplemental Experimental Procedures and can be found with this article online at doi:10.1016/j.devcel.2011.03.019.

## ACKNOWLEDGMENTS

We thank Takashi Araki, Kim Gallager, Brian Gregory, Mary Mullins, Scott Poethig, John Wagner, and Matthew Willmann for comments on the manuscript, Daniel Simola for help implementing the ROC analysis, Frank Wellmer for the *ap1 cal* 35S:LFY-GR seed, Gerco Angenent for the SEP3:SEP3-GFP seed, and Hao Yu for the *SEP3* in situ probe. This work was funded by NSF IOS 0849298 to D.W., NIH Training grants T32HG000046 (Computational Biology) and T32-HD007516 (Developmental Biology) to C.M.W., funding from Agri-Food Canada, Agricultural Bioproducts Innovation Program to R.S.A., and a JSPS fellowship to A.Y.

Received: October 8, 2010
Revised: March 5, 2011
Accepted: March 29, 2011
Published: April 18, 2011

## REFERENCES

Albani, M.C., and Coupland, G. (2010). Comparative analysis of flowering in annual and perennial plants. Curr. Top. Dev. Biol. *91*, 323–348.

Alon, U. (2007). Network motifs: theory and experimental approaches. Nat. Rev. Genet. *8*, 450–461.

Amasino, R. (2010). Seasonal and developmental timing of flowering. Plant J. *61*, 1001–1013.

Badis, G., Berger, M.F., Philippakis, A.A., Talukder, S., Gehrke, A.R., Jaeger, S.A., Chan, E.T., Metzler, G., Vedenko, A., Chen, X., et al. (2009). Diversity and complexity in DNA recognition by transcription factors. Science *324*, 1720–1723.

Bailey, T.L., and Elkan, C. (1995). The value of prior knowledge in discovering motifs with MEME. Proceedings/international conference on intelligent systems for molecular biology. ISMB *3*, 21–29.

Blazquez, M.A., Soowal, L.N., Lee, I., and Weigel, D. (1997). LEAFY expression and flower initiation in Arabidopsis. Development *124*, 3835–3844.

Blazquez, M.A., Ferrandiz, C., Madueno, F., and Parcy, F. (2006). How floral meristems are built. Plant Mol. Biol. *60*, 855–870.

Bowman, J.L., and Floyd, S.K. (2008). Patterning and polarity in seed plant shoots. Annu. Rev. Plant Biol. *59*, 67–88.

Burow, M., Halkier, B.A., and Kliebenstein, D.J. (2010). Regulatory networks of glucosinolates shape Arabidopsis thaliana fitness. Curr. Opin. Plant Biol. *13*, 348–353.

Busch, M.A., Bomblies, K., and Weigel, D. (1999). Activation of a floral homeotic gene in Arabidopsis. Science *285*, 585–587.

Calonje, M., Sanchez, R., Chen, L., and Sung, Z.R. (2008). EMBRYONIC FLOWER1 participates in polycomb group-mediated AG gene silencing in Arabidopsis. Plant Cell *20*, 277–291.

Chang, W.C., Li, C.W., and Chen, B.S. (2005). Quantitative inference of dynamic regulatory pathways via microarray data. BMC Bioinformatics *6*, 44.

Chen, L., Cheng, J.C., Castle, L., and Sung, Z.R. (1997). EMF genes regulate Arabidopsis inflorescence development. Plant Cell *9*, 2011–2024.

Clay, N.K., Adio, A.M., Denoux, C., Jander, G., and Ausubel, F.M. (2009). Glucosinolate metabolites required for an Arabidopsis innate immune response. Science *323*, 95–101.

de Folter, S., Urbanus, S.L., van Zuijlen, L.G., Kaufmann, K., and Angenent, G.C. (2007). Tagging of MADS domain proteins for chromatin immunoprecipitation. BMC Plant Biol. *7*, 47.

Denoux, C., Galletti, R., Mammarella, N., Gopalan, S., Werck, D., De Lorenzo, G., Ferrari, S., Ausubel, F.M., and Dewdney, J. (2008). Activation of defense response pathways by OGs and Flg22 elicitors in Arabidopsis seedlings. Mol. Plant *1*, 423–445.

Develey-Riviere, M.P., and Galiana, E. (2007). Resistance to pathogens and host developmental stage: a multifaceted relationship within the plant kingdom. New Phytol. *175*, 405–416.

Dodds, P.N., and Rathjen, J.P. (2010). Plant immunity: towards an integrated view of plant-pathogen interactions. Nat. Rev. Genet. *11*, 539–548.

Farnham, P.J. (2009). Insights from genomic profiling of transcription factors. Nat. Rev. Genet. *10*, 605–616.

Feys, B.J., Wiermer, M., Bhat, R.A., Moisan, L.J., Medina-Escobar, N., Neu, C., Cabral, A., and Parker, J.E. (2005). Arabidopsis SENESCENCE-ASSOCIATED GENE101 Stabilizes and Signals within an ENHANCED DIEASE SUSCEPTIBILITY1 Complex in Plant Innate Immunity. Plant Cell *17*, 2601–2613.

García, A.V., Blanvillain-Baufumé, S., Huibers, R.P., Wiermer, M., Li, G., Gobbato, E., Rietz, S., and Parker, J.E. (2010). Balanced nuclear and cytoplasmic activities of EDS1 are required for a complete plant innate immune response. PLoS Pathog. *6*, e1000970.

Gomez-Gomez, L., Felix, G., and Boller, T. (1999). A single locus determines sensitivity to bacterial flagellin in Arabidopsis thaliana. Plant J. *18*, 277–284.

Goodrich, J., Puangsomlee, P., Martin, M., Long, D., Meyerowitz, E.M., and Coupland, G. (1997). A Polycomb-group gene regulates homeotic gene expression in Arabidopsis. Nature *385*, 44–51.

Guilfoyle, T.J., and Hagen, G. (2007). Auxin response factors. Curr. Opin. Plant Biol. *10*, 453–460.

Hames, C., Ptchelkine, D., Grimm, C., Thevenon, E., Moyroud, E., Gerard, F., Martiel, J.L., Benlloch, R., Parcy, F., and Muller, C.W. (2008). Structural basis for LEAFY floral switch function and similarity with helix-turn-helix proteins. EMBO J. *27*, 2628–2637.

Heil, M. (2002). Ecological costs of induced resistance. Curr. Opin. Plant Biol. *5*, 345–350.

Hempel, F.D., Weigel, D., Mandel, M.A., Ditta, G., Zambryski, P.C., Feldman, L.J., and Yanofsky, M.F. (1997). Floral determination and expression of floral regulatory genes in Arabidopsis. Development *124*, 3845–3853.

Herms, D.A., and Mattson, W.J. (1992). The dilemma of plants - to grow or defend. Q. Rev. Biol. *67*, 283–335.

Hill, T.A., Day, C.D., Zondlo, S.C., Thackeray, A.G., and Irish, V.F. (1998). Discrete spatial and temporal cis-acting elements regulate transcription of the Arabidopsis floral homeotic gene APETALA3. Development *125*, 1711–1721.

Hollenhorst, P.C., Chandler, K.J., Poulsen, R.L., Johnson, W.E., Speck, N.A., and Graves, B.J. (2009). DNA specificity determinants associate with distinct transcription factor functions. PLoS Genet. *5*, e1000778.

Honma, T., and Goto, K. (2000). The Arabidopsis floral homeotic gene PISTILLATA is regulated by discrete cis-elements responsive to induction and maintenance signals. Development *127*, 2021–2030.

Hughes, J.D., Estep, P.W., Tavazoie, S., and Church, G.M. (2000). Computational identification of cis-regulatory elements associated with groups of functionally related genes in Saccharomyces cerevisiae. J. Mol. Biol. *296*, 1205–1214.

Irish, V.F. (2010). The flowering of Arabidopsis flower development. Plant J. *61*, 1014–1028.

Jack, T. (2004). Molecular and genetic mechanisms of floral control. Plant Cell *16*, S1–S17.

Ji, H., Jiang, H., Ma, W., Johnson, D.S., Myers, R.M., and Wong, W.H. (2008). An integrated software system for analyzing ChIP-chip and ChIP-seq data. Nat. Biotechnol. *26*, 1293–1300.

Kaufmann, K., Muino, J.M., Jauregui, R., Airoldi, C.A., Smaczniak, C., Krajewski, P., and Angenent, G.C. (2009). Target genes of the MADS transcription factor SEPALLATA3: integration of developmental and hormonal pathways in the Arabidopsis flower. PLoS Biol. *7*, e1000090.

Kaufmann, K., Wellmer, F., Muino, J.M., Ferrier, T., Wuest, S.E., Kumar, V., Serrano-Mislata, A., Madueno, F., Krajewski, P., Meyerowitz, E.M., et al. (2010). Orchestration of floral initiation by APETALA1. Science *328*, 85–89.

Kim, D.H., Doyle, M.R., Sung, S., and Amasino, R.M. (2009). Vernalization: winter and the timing of flowering in plants. Annu. Rev. Cell Dev. Biol. *25*, 277–299.

Kim, M.G., and Mackey, D. (2008). Measuring cell-wall-based defenses and their effect on bacterial growth in Arabidopsis. Methods Mol. Biol. *415*, 443–452.

Kobayashi, Y., and Weigel, D. (2007). Move on up, it's time for change mobile signals controlling photoperiod-dependent flowering. Genes Dev. *21*, 2371–2384.

Komeda, Y. (2004). Genetic regulation of time to flower in Arabidopsis thaliana. Annu. Rev. Plant Biol. *55*, 521–535.

Krizek, B.A., and Fletcher, J.C. (2005). Molecular mechanisms of flower development: an armchair guide. Nat. Rev. Genet. *6*, 688–698.

Kwon, C.S., Chen, C., and Wagner, D. (2005). WUSCHEL is a primary target for transcriptional regulation by SPLAYED in dynamic control of stem cell fate in Arabidopsis. Genes Dev. *19*, 992–1003.

Lamb, R.S., Hill, T.A., Tan, Q.K., and Irish, V.F. (2002). Regulation of APETALA3 floral homeotic gene expression by meristem identity genes. Development *129*, 2079–2086.

Liu, C., Thong, Z., and Yu, H. (2009a). Coming into bloom: the specification of floral meristems. Development *136*, 3379–3391.

Liu, C., Xi, W., Shen, L., Tan, C., and Yu, H. (2009b). Regulation of flower patterning by flowering time genes. Dev. Cell *16*, 711–722.

Liu, X., Brutlag, D.L., and Liu, J.S. (2001). BioProspector: discovering conserved DNA motifs in upstream regulatory regions of co-expressed genes. Pac. Symp. Biocomput. *2001*, 127–138.

Luscombe, N.M., Babu, M.M., Yu, H.Y., Snyder, M., Teichmann, S.A., and Gerstein, M. (2004). Genomic analysis of regulatory network dynamics reveals large topological changes. Nature *431*, 308–312.

Maizel, A., Busch, M.A., Tanahashi, T., Perkovic, J., Kato, M., Hasebe, M., and Weigel, D. (2005). The floral regulator LEAFY evolves by substitutions in the DNA binding domain. Science *308*, 260–263.

McClintick, J.N., and Edenberg, H.J. (2006). Effects of filtering by present call on analysis of microarray experiments. BMC Bioinformatics *7*, 49.

Michaels, S.D. (2009). Flowering time regulation produces much fruit. Curr. Opin. Plant Biol. *12*, 75–80.

Moyroud, E., Kusters, E., Monniaux, M., Koes, R., and Parcy, F. (2010). LEAFY blossoms. Trends Plant Sci. *15*, 346–352.

Mutasa-Gottgens, E., and Hedden, P. (2009). Gibberellin as a factor in floral regulatory networks. J. Exp. Bot. *60*, 1979–1989.

Nurmberg, P.L., Knox, K.A., Yun, B.W., Morris, P.C., Shafiei, R., Hudson, A., and Loake, G.J. (2007). The developmental selector AS1 is an evolutionarily conserved regulator of the plant immune response. Proc. Natl. Acad. Sci. USA *104*, 18795–18800.

Oh, S., Park, S., and van Nocker, S. (2008). Genic and global functions for Paf1C in chromatin modification and gene expression in Arabidopsis. PLoS Genet. *4*, e1000077.

Parcy, F. (2005). Flowering: a time for integration. Int. J. Dev. Biol. *49*, 585–593.

Parcy, F., Nilsson, O., Busch, M.A., Lee, I., and Weigel, D. (1998). A genetic framework for floral patterning. Nature *395*, 561–566.

Parcy, F., Bomblies, K., and Weigel, D. (2002). Interaction of LEAFY, AGAMOUS and TERMINAL FLOWER1 in maintaining floral meristem identity in Arabidopsis. Development *129*, 2519–2527.

Pavesi, G., Mauri, G., and Pesole, G. (2001). An algorithm for finding signals of unknown length in DNA sequences. Bioinformatics *17* (*Suppl 1*), S207–S214.

Poethig, R.S. (2003). Phase change and the regulation of developmental timing in plants. Science *301*, 334–336.

Roux, F., Touzet, P., Cuguen, J., and Le Corre, V. (2006). How to be early flowering: an evolutionary perspective. Trends Plant Sci. *11*, 375–381.

Ruiz-Garcia, L., Madueno, F., Wilkinson, M., Haughn, G., Salinas, J., and Martinez-Zapater, J.M. (1997). Different roles of flowering-time genes in the activation of floral initiation genes in Arabidopsis. Plant Cell *9*, 1921–1934.

Saddic, L.A., Huvermann, B., Bezhani, S., Su, Y., Winter, C.M., Kwon, C.S., Collum, R.P., and Wagner, D. (2006). The LEAFY target LMI1 is a meristem identity regulator and acts together with LEAFY to regulate expression of CAULIFLOWER. Development *133*, 1673–1682.

Schmid, M., Davison, T.S., Henz, S.R., Pape, U.J., Demar, M., Vingron, M., Scholkopf, B., Weigel, D., and Lohmann, J.U. (2005). A gene expression map of Arabidopsis thaliana development. Nat. Genet. *37*, 501–506.

Schmid, M., Uhlenhaut, N.H., Godard, F., Demar, M., Bressan, R., Weigel, D., and Lohmann, J.U. (2003). Dissection of floral induction pathways using global expression analysis. Development *130*, 6001–6012.

Schommer, C., Palatnik, J.F., Aggarwal, P., Chetelat, A., Cubas, P., Farmer, E.E., Nath, U., and Weigel, D. (2008). Control of jasmonate biosynthesis and senescence by miR319 targets. PLoS Biol. *6*, e230.

Schuettengruber, B., and Cavalli, G. (2009). Recruitment of polycomb group complexes and their role in the dynamic regulation of cell fate choice. Development *136*, 3531–3542.

Sing, A., Pannell, D., Karaiskakis, A., Sturgeon, K., Djabali, M., Ellis, J., Lipshitz, H.D., and Cordes, S.P. (2009). A vertebrate Polycomb response element governs segmentation of the posterior hindbrain. Cell *138*, 885–897.

Smyth, G.K. (2004). Linear models and empirical bayes methods for assessing differential expression in microarray experiments. Stat. Appl. Genet. Mol. Biol. *3*, Article3.

Steeves, T.A., and Sussex, I. (1989). Pattern in Plant Development (Cambridge, UK: Cambridge University Press).

Tapscott, S.J. (2005). The circuitry of a master switch: Myod and the regulation of skeletal muscle gene transcription. Development *132*, 2685–2695.

Thijs, G., Lescot, M., Marchal, K., Rombauts, S., De Moor, B., Rouze, P., and Moreau, Y. (2001). A higher-order background model improves the detection of promoter regulatory elements by Gibbs sampling. Bioinformatics *17*, 1113–1122.

Tian, D., Traw, M.B., Chen, J.Q., Kreitman, M., and Bergelson, J. (2003). Fitness costs of R-gene-mediated resistance in Arabidopsis thaliana. Nature *423*, 74–77.

Tornero, P., and Dangl, J.L. (2001). A high-throughput method for quantifying growth of phytopathogenic bacteria in Arabidopsis thaliana. Plant J. *28*, 475–481.

Turck, F., Fornara, F., and Coupland, G. (2008). Regulation and identity of florigen: FLOWERING LOCUS T moves center stage. Annu. Rev. Plant Biol. *59*, 573–594.

Turck, F., Roudier, F., Farrona, S., Martin-Magniette, M.L., Guillaume, E., Buisine, N., Gagnot, S., Martienssen, R.A., Coupland, G., and Colot, V. (2007). Arabidopsis TFL2/LHP1 specifically associates with genes marked by trimethylation of histone H3 lysine 27. PLoS Genet. *3*, e86.

van Zanten, M., Snoek, L.B., Proveniers, M.C.G., and Peeters, A.J.M. (2009). The many functions of ERECTA. Trends Plant Sci. *14*, 214–218.

Vlot, A.C., Liu, P.P., Cameron, R.K., Park, S.W., Yang, Y., Kumar, D., Zhou, F.S., Padukkavidana, T., Gustafsson, C., Pichersky, E., et al. (2008). Identification of likely orthologs of tobacco salicylic acid-binding protein 2 and their role in systemic acquired resistance in Arabidopsis thaliana. Plant J. *56*, 445–456.

Wagner, D., Sablowski, R.W., and Meyerowitz, E.M. (1999). Transcriptional activation of APETALA1 by LEAFY. Science *285*, 582–584.

Weigel, D., and Meyerowitz, E.M. (1993). Activation of floral homeotic genes in Arabidopsis. Science *261*, 1723–1726.

Weigel, D., and Nilsson, O. (1995). A developmental switch sufficient for flower initiation in diverse plants. Nature *377*, 495–500.

Weigel, D., Alvarez, J., Smyth, D.R., Yanofsky, M.F., and Meyerowitz, E.M. (1992). LEAFY controls floral meristem identity in Arabidopsis. Cell *69*, 843–859.

Wellmer, F., Alves-Ferreira, M., Dubois, A., Riechmann, J.L., and Meyerowitz, E.M. (2006). Genome-wide analysis of gene expression during early Arabidopsis flower development. PLoS Genet. *2*, e117.

William, D.A., Su, Y., Smith, M.R., Lu, M., Baldwin, D.A., and Wagner, D. (2004). Genomic identification of direct target genes of LEAFY. Proc. Natl. Acad. Sci. USA *101*, 1775–1780.

Wu, Z., Irizarry, R.A., Gentleman, R., Martinez-Murillo, F., and Spencer, F. (2004). A model based background adjustment for oligonucleotide expression arrays. J. Am. Stat. Assoc. *99*, 909–917.

Yamaguchi, A., Wu, M.F., Yang, L., Wu, G., Poethig, R.S., and Wagner, D. (2009). The microRNA-regulated SBP-Box transcription factor SPL3 is a direct upstream activator of LEAFY, FRUITFULL, and APETALA1. Dev. Cell *17*, 268–278.

Yamamoto, Y.Y., Yoshitsugu, T., Sakurai, T., Seki, M., Shinozaki, K., and Obokata, J. (2009). Heterogeneity of Arabidopsis core promoters revealed by high-density TSS analysis. Plant J. *60*, 350–362.

Yant, L., Mathieu, J., and Schmid, M. (2009). Just say no: floral repressors help Arabidopsis bide the time. Curr. Opin. Plant Biol. *12*, 580–586.

Zipfel, C., Robatzek, S., Navarro, L., Oakeley, E.J., Jones, J.D., Felix, G., and Boller, T. (2004). Bacterial disease resistance in Arabidopsis through flagellin perception. Nature *428*, 764–767.